

Electronic states in coupled random chains

Youyan Liu* and K. A. Chao

Department of Physics and Measurement Technology, University of Linköping, S-58183 Linköping, Sweden

(Received 29 July 1985)

Using a matrix representation we have generalized the single-chain site-decimation method to the coupled-chain block-decimation method, and used it to renormalize the Green's-function equation of motion for coupled random chains. The density of states and the localization length are investigated by this method.

A system of weakly coupled disordered chains of atoms is classified as quasi-one-dimensional. However, the weak interchain coupling has been ignored in most of the existing theoretical analyses. While this zeroth-order approximation can provide reliable information for certain physical properties, it often gives doubtful answers. For instance, the hopping of an electron in a single chain of atoms containing impurities must be quite different from that in a system of many such chains weakly coupled together. When the hopping along one chain is hindered by an impurity, it can find a bypass through the neighboring chains.

Very little is known about the electronic properties of quasi-one-dimensional disordered systems, since the simpler one-dimensional disordered systems are already difficult enough. In recent years many authors have studied one-dimensional disordered systems with numerical methods based on the recursion formula^{1,2} of Haydock *et al.*³ or on real-space renormalization techniques.⁴⁻⁹ These approaches yield very accurate results with a reasonable amount of computer time. In this paper we will generalize the real-space renormalization decimation scheme and use it to study coupled random chains.

We consider a finite number (N) of coupled chains labeled by the chain index $\mu = 1, 2, \dots, N$. Each chain consists of an infinite number of sites with the site index $i = -\infty, \dots, -1, 0, 1, \dots, \infty$. Let $\epsilon(\mu)_i$ be the site energy and $t(\mu, \nu)_{ij}$ the hopping from the j th site in the ν th chain to the i th site in the μ th chain. If $(\mu, i) = (\nu, j)$, we define $t(\mu, \mu)_{ii} = 0$. Both $\epsilon(\mu)_i$ and $t(\mu, \nu)_{ij}$ can be random numbers. Then the Hamiltonian is expressed as

$$H = \sum_{\mu, i} \epsilon(\mu)_i c_{\mu i}^\dagger c_{\mu i} + \sum_{\mu, \nu, i, j} t(\mu, \nu)_{ij} c_{\mu i}^\dagger c_{\nu j} . \tag{1}$$

By imposing a finite range on the hopping, $t(\mu, \nu)_{ij} = 0$ if $|i - j| > M$, we can divide the system into an infinite number of blocks, the size of which is $N \times M$. The site (μ, k) belongs to the I th block if $IM < k \leq (I+1)M$. In terms of these blocks the Hamiltonian can be rewritten as

$$H = \sum_I H_I + \sum_I (H_{I, I+1} + H_{I, I-1}) . \tag{2}$$

The I th block is described by

$$H_I = \sum_{\mu} \sum_{i=1}^M \epsilon(\mu)_{IM+i} c_{\mu, IM+i}^\dagger c_{\mu, IM+i} + \sum_{\mu, \nu} \sum_{i, j=1}^M t(\mu, \nu)_{IM+i, IM+j} c_{\mu, IM+i}^\dagger c_{\nu, IM+j} . \tag{3}$$

It is easy to see that the only hoppings between blocks are the nearest-neighbor-block hoppings which are described by

$$H_{I, I\pm 1} = \sum_{\mu, \nu} \sum_{i, j=1}^M t(\mu, \nu)_{IM+i, (I\pm 1)M+j} \times c_{\mu, IM+i}^\dagger c_{\nu, (I\pm 1)M+j} . \tag{4}$$

For a fixed value of I there are NM sites at $(\mu, IM+i)$ with $\mu = 1, 2, \dots, N$ and $i = 1, 2, \dots, M$. We will enumerate these sites by counting first $\mu = 1$ and $i = 1, 2, \dots, M$, and then $\mu = 2$ and $i = 1, 2, \dots, M$, and so on, as shown in Fig. 1. These NM sites in the I th block can now be labeled as (I, p) with $p = 1, 2, \dots, NM$. Similarly, we can rewrite the site energies and the hopping integrals in the new notations as

$$\epsilon(\mu)_{IM+i} \Rightarrow \epsilon(I)_p, \quad p = (\mu - 1)M + i ,$$

and

$$t(\mu, \nu)_{IM+i, JM+j} \Rightarrow t(I, J)_{pq} ,$$

$$p = (\mu - 1)M + i \text{ and } q = (\nu - 1)M + j .$$

Then, (3) and (4) can be simplified as

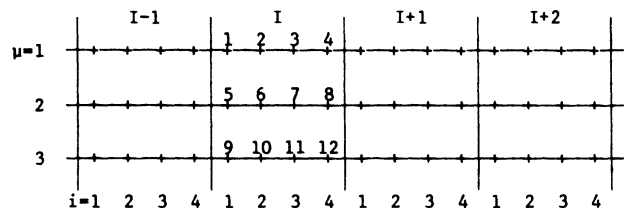


FIG. 1. An illustrative example for relabeling the sites in the I th block of size $N = 3$ and $M = 4$.

$$H_I = \sum_p \epsilon(I)_p [c(I)_p]^\dagger c(I)_p + \sum_{p,q} t(I,I)_{pq} [c(I)_p]^\dagger c(I)_q, \quad (5)$$

$$H_{I,I\pm 1} = \sum_{p,q} t(I,I\pm 1)_{pq} [c(I)_p]^\dagger c(I\pm 1)_q. \quad (6)$$

Let $|I_p\rangle$ be the localized state at the (I,p) site. With respect to this localized basis

$$\{|I_p\rangle; I = -\infty, \dots, 0, \dots, \infty; p = 1, 2, \dots, NM\},$$

the matrix representation of the operators H_I and $H_{I,I\pm 1}$ are

$$\begin{aligned} \hat{H}(I)_{pq} &= |I_p\rangle \epsilon(I)_p \langle I_p| \quad \text{if } p=q, \\ &= |I_p\rangle t(I,I)_{pq} \langle I_q| \quad \text{if } p \neq q, \end{aligned} \quad (7)$$

and

$$\hat{H}(I, I\pm 1)_{pq} = |I_p\rangle t(I, I\pm 1)_{pq} \langle I\pm 1, q|. \quad (8)$$

The matrix representation of the Green's-function operator can be put in the similar form

$$\hat{G}(I, J)_{pq} = |I_p\rangle \left\langle I_p \left| \frac{1}{z\mathbf{1} - H} \right| J_q \right\rangle \langle J_q|, \quad (9)$$

where $z = E + i\eta$ is the complex eigenenergy and $\mathbf{1}$ is the unit operator. The equation of motion for the Green's function,

$$z\hat{G} = \hat{\mathbf{1}} + \hat{H}\hat{G}, \quad (10)$$

can then be expressed in the matrix form as

$$\begin{aligned} [z\hat{\mathbf{1}} - \hat{H}(I)]\hat{G}(I, J) &= \hat{\mathbf{1}}\delta_{IJ} + \sum_K \hat{H}(I, K)\hat{G}(K, J) \\ &= \hat{\mathbf{1}}\delta_{IJ} + \hat{H}(I, I-1)\hat{G}(I-1, J) \\ &\quad + \hat{H}(I, I+1)\hat{G}(I+1, J). \end{aligned} \quad (11)$$

With the blocks playing the roles of single sites, Eqs. (2) and (11) have exactly the same forms as their counterparts in the single-chain tight-binding Anderson model with nearest-neighbor-site hopping. Consequently, similar to site decimation, here we can introduce block decimation to derive the recursion relation for renormalization. The method is well known, so we will only write down the recursion relation for $\hat{G}(I, I)$ which will be used to calculate the density of states. After α renormalizations the results are

$$[z\hat{\mathbf{1}} - \hat{H}^\alpha(I)]\hat{G}^\alpha(I, I) = \hat{\mathbf{1}} + \hat{H}^\alpha(I, I-1)\hat{G}^\alpha(I-1, I) + \hat{H}^\alpha(I, I+1)\hat{G}^\alpha(I+1, I), \quad (12)$$

$$\begin{aligned} \hat{H}^\alpha(I) &= \hat{H}^{\alpha-1}(I) + \hat{H}^{\alpha-1}(I, I-1)[z\hat{\mathbf{1}} - \hat{H}^{\alpha-1}(I-1)]^{-1}\hat{H}^{\alpha-1}(I-1, I) \\ &\quad + \hat{H}^{\alpha-1}(I, I+1)[z\hat{\mathbf{1}} - \hat{H}^{\alpha-1}(I+1)]^{-1}\hat{H}^{\alpha-1}(I+1, I), \end{aligned} \quad (13)$$

and

$$\hat{H}^\alpha(I, I\pm 1) = \hat{H}^{\alpha-1}(I, I\pm 1)[z\hat{\mathbf{1}} - \hat{H}^{\alpha-1}(I\pm 1)]^{-1}\hat{H}^{\alpha-1}(I\pm 1, I\pm 2). \quad (14)$$

Since the site energies $\epsilon(I)_p$ and the hopping integrals $t(I, J)_{pq}$ are random numbers, the above recursion relations are for a given configuration specified by the values of the site energies and the hopping integrals. When the blocks are decimated, all possible configurations of the decimated blocks must be taken into account. Let $\Pi(I)_\xi$ be the probability that the I th block is in the ξ th configuration. The configuration average over the $(I\pm 1)$ th block in (13) and (14) leads to

$$\begin{aligned} \hat{H}^\alpha(I) &= \hat{H}^{\alpha-1}(I) + \sum_\xi \Pi(I-1)_\xi \hat{H}^{\alpha-1}(I, I-1)[z\hat{\mathbf{1}} - \hat{H}^{\alpha-1}(I-1)]^{-1}\hat{H}^{\alpha-1}(I-1, I) \\ &\quad + \sum_\xi \Pi(I+1)_\xi \hat{H}^{\alpha-1}(I, I+1)[z\hat{\mathbf{1}} - \hat{H}^{\alpha-1}(I+1)]^{-1}\hat{H}^{\alpha-1}(I+1, I) \end{aligned} \quad (15)$$

and

$$\hat{H}^\alpha(I, I\pm 1) = \sum_\xi \Pi(I\pm 1)_\xi \hat{H}^{\alpha-1}(I, I\pm 1)[z\hat{\mathbf{1}} - \hat{H}^{\alpha-1}(I\pm 1)]^{-1}\hat{H}^{\alpha-1}(I\pm 1, I\pm 2). \quad (16)$$

The effective coupling $\hat{H}^\alpha(I, I\pm 1)$ gets weaker after each renormalization. As $\alpha \rightarrow \infty$ the fixed point is determined from $\hat{H}^\alpha(I, I\pm 1) = 0$. The Green's function $\hat{G}(I, I)$ for the ξ th configuration of the I th block is then diagonalized and expressed as

$$\hat{G}(z; I)_\xi \equiv \lim_{\alpha \rightarrow \infty} \hat{G}^\alpha(I, I) = \lim_{\alpha \rightarrow \infty} [z\hat{\mathbf{1}} - \hat{H}^\alpha(I)]^{-1}. \quad (17)$$

From the configuration-averaged Green's function

$$\hat{G}(z; I) = \sum_\xi \Pi(I)_\xi \hat{G}(z; I)_\xi, \quad (18)$$

we can calculate the density of states

$$\rho(E) = -\frac{1}{\pi} \lim_{\eta \rightarrow 0} \text{Im Tr} \hat{G}(E + i\eta; I). \quad (19)$$

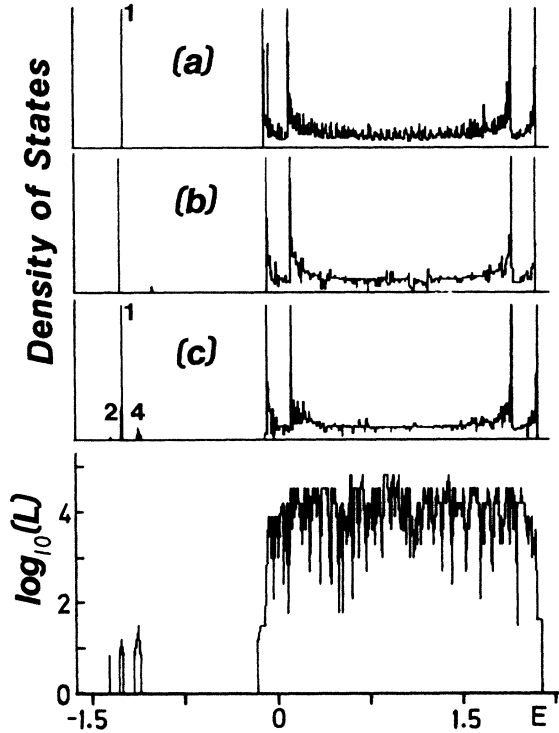


FIG. 2. The DOS and the localization length for $x=0.01$. (a) 500-atom exact solution, (b) $M=1$ renormalization result, and (c) $M=2$ renormalization result.

Although the above analysis is valid for an arbitrary size of the block, in this paper we will only present the results for two coupled chains with both nearest-neighbor interchain and nearest-neighbor intrachain hoppings. However, we should point out that even for only the

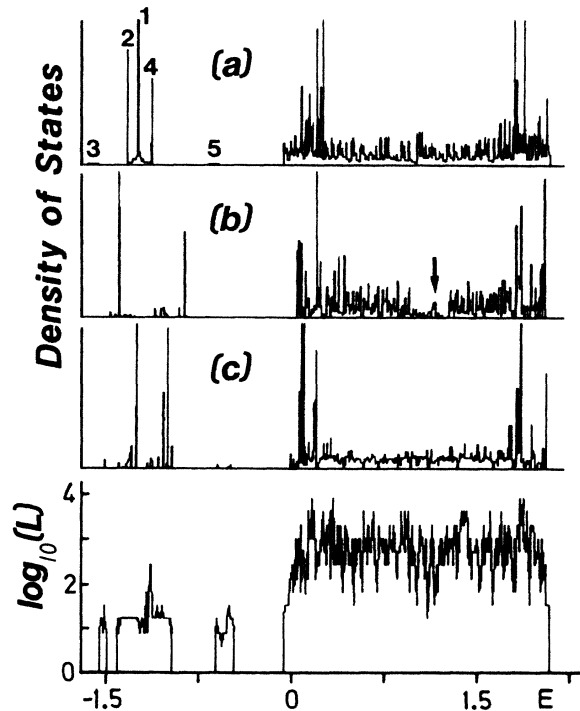


FIG. 3. Same as Fig. 2 for $x=0.1$.

nearest-neighbor intrachain hopping, it is important to choose the longitudinal dimension of the block M greater than 1 in order to obtain the correct localized cluster states. Since each configuration of the block is calculated separately, cluster states of the size $N \times M$ are treated exactly. Therefore, in our calculation we fix $N=2$ but increase the value of M to achieve convergent results.

We consider a simple random $A_{1-x}B_x$ alloy. The site energy of the A atoms is $E_A=1$ and of the B atoms is $E_B=-1$. The nearest-neighbor hopping is $t(\mu, \mu)_{i, i \pm 1} = -0.5$ for intrachain and $t(1, 2)_{ii} = t(2, 1)_{ii} = -0.1$ for interchain hopping. We have computed the density of states (DOS) for three values of $x=0.01, 0.1$, and 0.5 . For each case we also compare our calculation to the exact solution which is obtained by first simulating a random alloy of 500 atoms and then solving the eigenvalue problem numerically.

Figure 2 shows the DOS for $x=0.01$. Part (a) is the 500-atom exact solution, consisting of a continuous spectrum for extended states and a sharp low-energy peak marked as peak 1. From the corresponding eigenfunction we can identify the origin of this peak 1 as a single isolated B atom. The probability of having a pair of nearest-neighbor B atoms is $x^2=0.0001$. Therefore, for a finite system of 500 atoms, such a pair does not appear.

Parts (b) and (c) of Fig. 1 are the block-renormalization results for block size $M=1$ and 2 , respectively. At the stage $M=2$ the continuous spectrum already converges to the exact solution. However, in the low-energy region, not only is peak 1 slightly broadened, but also two new peaks, 2 and 4, appear. Later we will prove that these two new peaks are due to a pair of nearest-neighbor B atoms.

For numerical calculation the fixed point is reached when the effective coupling $\hat{H}^\alpha(I, I \pm 1)$ becomes smaller than the numerical lower bound of the computer. For given energy E this occurs at different values of $\alpha(E)$. We can define a "localization length"

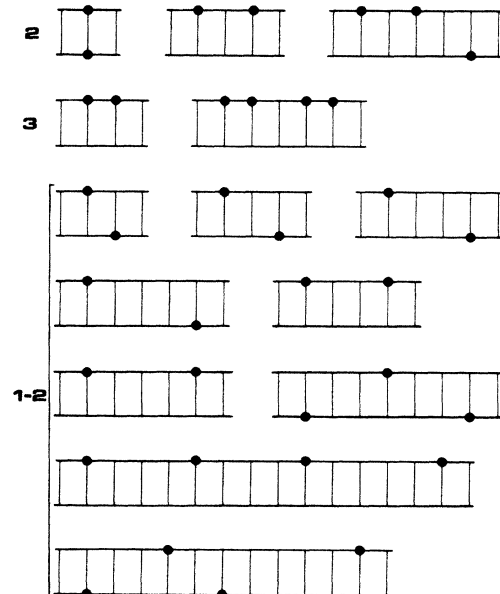


FIG. 4. Clusters of B atoms (marked by large dots) in a computer-simulated two-chain 500-atom system for $x=0.1$.

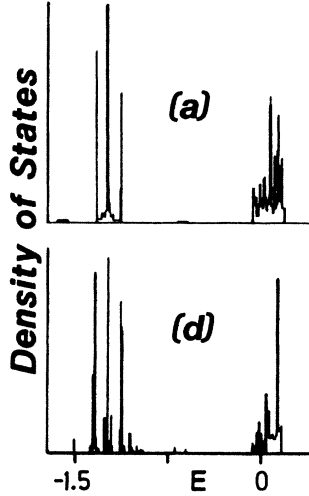


FIG. 5. The DOS for $x=0.1$. (a) 500-atom exact solution, and (d) $M=3$ renormalization result. Only the lower-energy part of the spectrum is shown.

$$L(E) = M2^{\alpha(E)} \quad (20)$$

as a relative measure of the electron localization. At the bottom of Fig. 2 we have shown the behavior of $\log_{10}L(E)$ for the whole spectrum.

Similar plots are given in Fig. 3 for $x=0.1$. The low-energy part of the exact solution [part (a)] from peak 3 to peak 5 corresponds to various types of cluster states. Peak 1 is caused by an isolated B atom as we have mentioned before. The other kinds of clusters of B atoms which we can identify for the exact solution are shown in Fig. 4. The lattice site is occupied by a B atom if it is

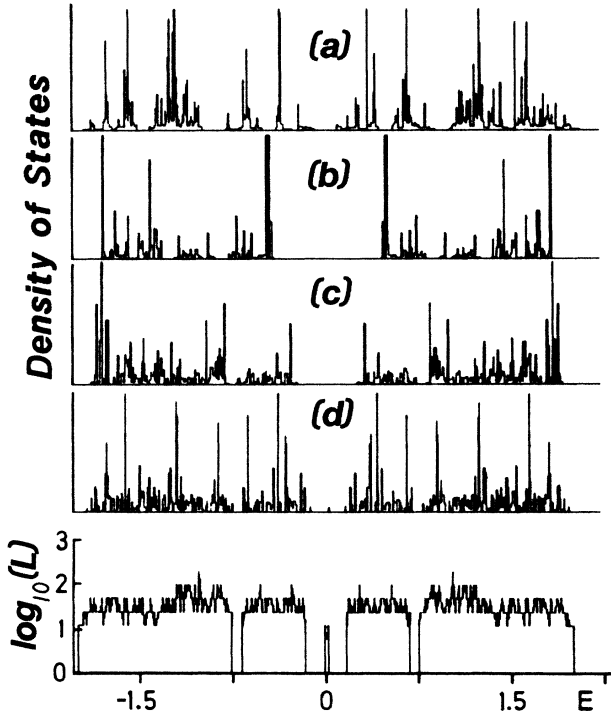


FIG. 6. The DOS and the localization length for $x=0.5$. (a) 500-atom exact solution, (b) $M=1$ renormalization result, (c) $M=2$ renormalization result, and (d) $M=3$ renormalization result.

marked by a large dot. Otherwise, it is occupied by an A atom. The bonding and the antibonding orbitals of the three clusters in row 2 of Fig. 4 produce, respectively, peak 2 and peak 4 of exact solution. Similarly, peaks 3 and 5 of the exact solution are due to the two clusters in row 3 of Fig. 4. The rest of the clusters in Fig. 4, grouped into 1-2, can be considered as either larger clusters or collections of interacting smaller clusters of B atoms. This group 1-2 is responsible to the states between peaks 1 and 2, and between peaks 1 and 4 of the exact solution.

Peak 2 and 4 in Fig. 2 for $x=0.01$ have exactly the same energies as those in Fig. 3, and hence are caused by a pair of interchain nearest-neighbor B atoms. The slight broadening of peak 1 in part (c) of Fig. 2 is now understood as due to the weak interaction between clusters.

Let us return to Fig. 3. The large change of the continuous spectrum from part (b) (for $M=1$) to part (c) (for $M=2$) is indicated by an arrow. Therefore, the cluster states have a sizable effect on the whole spectrum. If we compare parts (a) and (c) in Fig. 3, we see the significant difference in the low-energy region and around the edges of the continuous spectrum. We then continue to calculate these parts of the spectrum with larger block $M=3$. The results are shown in Fig. 5 as part (d). This stage of computation not only reproduces the detailed features of the 500-atom exact solution, but also reveals the rich structure as a result of the interaction between clusters.

The localization length L is shown at the bottom of Fig. 3. If we compare it to its counterpart in Fig. 2, we see that as x increases, the localization length gets shorter in the continuous-spectrum region, but longer in the discrete spectrum region. This is what one would expect.

For $x=0.5$, the system is a homogeneous mixture of equal amount of A and B atoms. Since one can no longer define the clusters of B atoms in a host of A atoms, the properties of the system are not dominated by the inhomogeneous distribution of clusters of B atoms. Consequently, convergent results can be derived without using very large block. This is indeed what we have found. In Fig. 6, when the block size increases from $M=1$ [part (b)] to $M=2$ [part (c)] and to $M=3$ [part (d)], the DOS has already exhibited all the features of the 500-atom exact solution [part (a)]. We have checked that part (d) is the convergent result. We also see that for the whole spectrum the localization length is between 100 and 200 lattice constants.

It is important to mention that depending on the value of $t(\mu, \nu)_{ij}$ and the number N of coupled chains, one may need a very large block size (large value of M) in order to obtain convergent results. It seems that there is no simple way to estimate the critical size of the block for given $t(\mu, \nu)_{ij}$ and N . The convergence has to be checked separately for each individual case.

To close this paper, we would like to emphasize that not only $\hat{G}(I, I)$, but also $\hat{G}(I, J)$ with $I \neq J$ can be derived from (11) by block renormalization.

The work was financially supported by the Swedish Natural Science Research Council under Grants No. NFR F-FU 3996-127 and No. NFR S-FO 3996-130.

*Permanent address: Department of Physics, South China Institute of Technology, Guangzhou, People's Republic of China.

¹M. Weissmann and N. V. Cohan, *J. Phys. C* **8**, 109 (1975).

²R. Day and F. Martino, *J. Phys. C* **14**, 4247 (1981).

³R. Haydock, V. Heine, and M. J. Kelly, *J. Phys. C* **8**, 2591 (1975).

⁴H. Aoki, *Solid State Commun.* **31**, 999 (1979).

⁵B. Koiller, M. O. Robbins, M. A. Davidovich, and C. E. T.

Goncalves da Silva, *Solid State Commun.* **45**, 955 (1983).

⁶M. O. Robbins and B. Koiller, *Phys. Rev. B* **27**, 7703 (1983).

⁷B. W. Southern, A. A. Kumar, and J. A. Ashraff, *Phys. Rev. B* **28**, 1785 (1983).

⁸C. Wiecko and E. Roman, *Phys. Rev. B* **30**, 1603 (1984).

⁹Youyan Liu, R. Riklund, and K. A. Chao, *J. Phys. C* **17**, L843 (1984).